ORIGINAL ARTICLE

Disulfiram-copper activates chloride currents and induces apoptosis with tyrosine kinase in prostate cancer cells

Wei Lei[1,*] | Jingkui Xu[2,*] | Yiyao Ya[1,*] | Jinxiang Zhang[1,*] | Xiuying Hou[2] | Qiliang Zhai[1] | Zeyu Zha[1] | Yangjia Zhuo[1] | You Zhou[1] | Hong Yuan[1] | Yuxiang Liang[1] | Zhaodong Han[1] | Weide Zhong[1] | Linyan Zhu[2] | Yehui Chen[1]

[1] Department of Urology, Guangzhou First People's Hospital, School of Medicine, South China University of Technology, Guangzhou, China

[2] Department of Physiology, School of Medicine, Jinan University, Guangzhou, China

Correspondence
Linyan Zhu, Department of Physiology, School of Medicine, Jinan University, Guangzhou, Guangdong, 510632, China.
Email: lyzhu@jnu.edu.cn
Yehui Chen, Department of Urology, Guangzhou First People's Hospital, School of Medicine, South China University of Technology, Guangzhou, Guangdong, 510013, China.
Email: eychenyh@scut.edu.cn

*These authors contributed equally to this work.

Abstract

Aim: To elucidates the mechanism that disulfiram/copper complex (DSF/Cu) treatment activates chloride channels and induces apoptosis in prostate cancer cells.

Methods: Cellular membrane currents were measured by membrane clamp technique; western blot to detect protein expression; flow cytometry to detect apoptosis; immunofluorescence to detect target protein co-localization, and further validated by a combination of protein-protein interaction and mock protein molecular docking techniques.

Results: DSF/Cu activated chloride channels and induced apoptosis in LNCaP (a type of androgen-dependent prostate cancer cells) cells. The chloride currents activated by DSF/Cu were significantly reduced after knockdown of CLC3 with siRNA. In addition, DSF/Cu-activated chloride currents were reduced to background current levels after perfusion with genistein, a highly specific tyrosine kinase inhibitor. Conversely, DSF/Cu failed to activate chloride currents in LNCaP cells after 30 minutes of pre-incubation with genistein. When genistein was removed, and DSF/Cu was added, the activated currents were small and unstable, and gradually decreased. Immunofluorescence in LNCaP cells also showed co-localization of the CLC3 protein with tyrosine kinase 2β (PTK2B).

Conclusion: DSF/Cu can activate chloride channels and induce apoptosis in LNCaP cells with the involvement of tyrosine kinase. These results provide new insights into the target therapy of prostate cancer.

KEYWORDS
apoptosis, chloride channels, DSF/Cu, prostate cancer, tyrosine kinase

1 | INTRODUCTION

Prostate cancer is one of the most common malignant tumors in males and originates from glandular epithelial cells.[1] The main clinical treatment for prostate cancer is androgen deprivation, which can be achieved by a radical prostatectomy (RP) or endocrine therapy.[2] A variety of endocrine therapy drugs have been developed in recent years. A study shows that the addition of abiraterone acetate and prednisone to androgen-deprivation therapy significantly increased overall survival and radiographic progression-free survival in castration-sensitive

prostate cancer.[3] The incidence of prostate cancer recurrence can be significantly decreased after RP,[4] and endocrine therapy can inhibit the level of androgen in the body for a therapeutic effect.[5] However, a significant percentage of patients experience recurrence and progressive transfer to refractory androgen independent prostate cancer within years after RP treatment, and the efficacy of endocrine therapy gradually declines over time. Although there is a lot of research on prostate cancer treatment, for example, some researchers have indicated that certain lncRNAs can suppress androgen resistance in prostate cancer.[6,7] Another study showed that AP4/L-plastin axis regulated by the phosphatidylinositol 3-kinase/protein kinase B (PI3K/AKT) pathway contributed to prostate cancer metastasis and castration resistance.[8] These studies are still in the basic stages. Therefore, there is an urgent need to find an affordable drug with highly efficient therapeutic effects to regulate androgen production for the treatment of prostate cancer.

Recent studies have shown that disulfiram (DSF) has antitumor effects and exhibits a selective antitumor effect after the chelation of metal ions. In breast cancer cells, DSF/Cu induces apoptosis by inhibiting proteasome activity both in vivo and in vitro.[9] Previous work has also shown that DSF/Cu induces MCF-7 breast cancer cells to accumulate in G2/M phase and induces apoptosis in a concentration-dependent manner.[10] DSF/Cu is selectively cytotoxic to CNE-2Z nasopharyngeal carcinoma cells and induces apoptosis via the CLC3 chloride channel pathway. In the context of prostate cancer, DSF has been identified as a potential therapeutic agent by high-throughput cellular screening of currently marketed drugs.[11]

DSF/Cu may mediate apoptosis through chloride ion channels.[12] As one of the main anion channels in human cells, chloride channels are involved in cell migration, growth and proliferation, volume regulation, apoptosis, and the regulation of other biological behaviors.[9,11,13]

Recent study showed that DSF/Cu-induced apoptosis in LNCaP cells correlates with intracellular oxidative stress and reactive oxygen species production.[14] However, whether chloride channels are involved in the DSF/Cu-induced apoptosis of LNCaP cells remains to be investigated. In this study, we used whole-cell patch-clamp techniques along with flow cytometry and immunofluorescence to investigate the mechanism of action of DSF/Cu on LNCaP cells, and results showed that chloride channels played a positive role in promoting apoptosis in LNCaP cells. These results provide a theoretical basis for the clinical use of DSF/Cu in prostate cancer.

2 | MATERIALS AND METHODS

2.1 | Drugs and reagents

DSF, $CuCl_2$ solid powder, 3-(4,5-dimethylthiazole-2)-2,5-diphenyltetrazolium bromide (MTT) powder 4,4′-diisothiocyanostibibene-2,2′-disulfonic acid (DIDS) powder and 5-nitro-2- (3-phenlpropylamino) benzoic acid (NPPB) powder were purchased from Sigma-Aldrich (St Louis, MO). Annexin V-FITC/PI apoptosis detection kits were purchased from KeyGEN BioTECH (Jiangsu, China).

2.2 | Cell culture

The human prostate cancer cell line LNCaP (Cellcook Biotech Co. Ltd, Guangzhou, China) was cultured in RPMI 1640 medium (Cellcook Biotech Co. Ltd, Guangzhou, China) with 10% FBS (Gibco, NY), 10^5 U/L penicillin and 100 mg/L streptomycin (Sigma-Aldrich) under a saturated humidified atmosphere of 37°C, 5% CO_2. Cells were passaged at intervals of 72 hours and detached with 0.25% trypsin-0.02% ethylene diamine tetraacetic acid (EDTA) (Sigma-Aldrich).

2.3 | Cell proliferation tests (MTT method)

LNCaP cells were inoculated in 96-well plates and incubated with different concentrations of DSF/Cu for 24 hours. Then, 20 μl MTT solution was added to each well for 4 hours. After removing the supernatant, DMSO was added, and plates were incubated at 37°C for 10 minutes. The plates with cells were observed using a microplate reader to detect absorbance at 490 nm.

2.4 | Whole-cell recordings

Cells were plated on 22 mm round coverslips and incubated for at least 30 minutes. Whole-cell recording experiments were performed with an electrode resistance of 5-10 MΩ with a probe filled with pipette solution under an extracellular patch clamp-7 (EPC-7) patch-clamp amplifier (HEKA, Darmstadt, Germany) at 20-24°C. Once the whole cell configuration was established, cells were held at the chloride equilibrium potential of 0 mV and then stepped repeatedly to 0, $\pm$ 40, and $\pm$ 80 mV with a 200 milliseconds duration for each step and 4 seconds intervals between steps. Electrophysiological signals were recorded by a computer via a laboratory interface (CED 1401, Cambridge, UK) with a sampling rate of 3 kHz.

2.5 | Apoptosis assays

After incubation in the indicated medium for a defined time, the cells were trypsinized using 0.25% trypsin without EDTA. The cells were then stained with an Annexin V-FITC/PI apoptosis detection kit following the manufacturer's instruction, and analyzed by a BD C6 flow cytometer (BD Accuri, Piscataway, NJ).

2.6 | Knockdown of CLC3 with siRNA

CLC3 siRNAs were synthesized and labeled with carboxyfluorescein by GenePhama (Gene Pharma, Shanghai, China) and stored at −20°C. The forward and reverse sequences of the CLC3 siRNA were 5′-CAA UGG AUU UCC UGU CAU ATT-3′ and 5′-UAU GACAGG AAA UCC AUU GTA-3′. At 30-50% confluence, the cells were transfected with 100 nM siRNA or negative control siRNA using siRNA-Mate at a 1 of 250 final dilution (GenePhama, Shanghai, China). The cells were cultured in normal medium, and after 48 hours the cells were subjected to whole cell recordings and western blot analysis.

2.7 | Western blot analysis

LNCaP cells were lysed with radio immunoprecipitation assay (RIPA) lysis buffer (Beyotime Biotechnology, Shanghai, China), and 30 mg (50 μg/μl) of protein was loaded onto SDS–PAGE gels (EpiZyme Biotech, Shanghai, China) for each sample and subsequently transferred to polyvinylidene fluoride (PVDF) membranes (0.45 mm, Millipore, Bedford, MA). The membranes were blocked at room temperature for 2 hours in 5% evaporated milk dissolved in tris buffered saline-Tween (TBST) (0.1% Tween-20, Sigma-Aldrich, St Louis, MO). Membranes were incubated overnight at 4°C with primary antibodies, including rabbit anti-CLC3 (1:100, 13359S, Cell Signaling, Danvers, MA) and rabbit anti-GAPDH (1:750, D16H11, Cell Signaling, Danvers, MA). The secondary horseradish peroxidase (HRP)-conjugated antibody was goat anti-rabbit IgG (H + L) (SA00001-2, Proteintech, Wuhan, China). The bands were detected with Western Blot Luminol Reagent (Santa Cruz, CA).

2.8 | Immunofluorescence detection

LNCaP cells were fixed with 4% paraformaldehyde containing 0.12 mol sucrose, permeabilized with 0.5% Triton X–100, and blocked with 1% goat serum albumin in PBS for 1 hour. Samples were then incubated at 4°C overnight with primary antibodies against CLC3 (rabbit polyclonal ab134285, 1:80, Abcam, Cambridge, UK) and PTK2B (rabbit monoclonal ab32571, 1:100, Abcam, Cambridge, UK). The CLC3 antibody was detected with Alexa Fluor 488-conjugated secondary antibodies (goat-anti mouse, 1:8000, Beyotime Biotechnology, Shanghai, China), and PTK2B antibodies were detected with Cy3-conjugated secondary antibodies (goat-anti rabbit, 1:8000, Beyotime Biotechnology, Shanghai, China). Samples were detected with a Nikon Eclipse C1 confocal laser-scanning microscope (Nikon Corporation, Tokyo, Japan).

2.9 | Statistical analysis

All quantitative data were presented as the mean ± standard deviations from at least three independent experiments. Chi-square tests (χ^2 tests) were used to assess the relationships between non-parametric variables, and the two-tailed Student's t-test or one-way ANOVA was used to evaluate the relationship between parametric variables. The threshold for statistical significance was set at $P < .05$. All statistical tests were performed with SPSS. (Version 19.0.; IBM Corp., Armonk, NY).

3 | RESULTS

3.1 | DSF/Cu activates chloride channels in LNCaP cells to produce chloride currents

The results of our previous studies suggested that DSF/Cu can activate chloride currents in multiple cell lines, so we tested whether DSF/Cu

also activates chloride currents in LNCaP cells. With a ± 80 mV voltage-clamp, the current density of LNCaP cells gradually increased to (69.79 ± 25.55) pA/pF (80 mV), (−45.57 ± 18.61) pA/pF (−80 mV) using an isotonic solution containing 400 nM of DSF/Cu (Figure 1A). However, the inward and outward currents were reduced to (6.04 ± 2.79) pA/pF (80 mV), and (−7.89 ± 2.65) pA/pF (−80 mV) after perfusion with the chloride channel inhibitor DIDS, with inward and outward currents suppression rates of (89.32 ± 3.10)% (80 mV) and (80.01 ± 1.38)% (−80 mV), respectively (Figures 1A-1E). After perfusion with the chloride channel inhibitor NPPB, the cell current density was reduced to (22.55 ± 6.40) pA/pF (80 mV), and (−18.70 ± 9.92) pA/pF (−80 mV), while the internal and external currents suppression rates were (64.85 ± 17.09)% (80 mV) and (57.42 ± 18.55)% (- 80 mV), respectively (Figures 1F-1J). According to the Nernst equation, the reversal potential is −0.91 mV, which is close to the theoretical value of the equilibrium potential of chloride ions under this experimental condition.[15] These results suggest that the DSF/Cu-activated LNCaP cells mainly produce chloride currents.

3.2 | DSF/Cu inhibits the growth and proliferation of LNCaP cells and induces apoptosis suppressed by NPPB and DIDS

Apoptosis is a highly regulated cellular process that is essential for cell and tissue development.[16] We determined that the IC$_{50}$ value of DSF/Cu for inhibition of LNCaP cell proliferation was 386.4 nM after 24 hours of culture (Figures 2A and 2B). According to the IC$_{50}$ value, the concentration of DSF/Cu was set at 400 nM in this study. To confirm whether chloride channels are involved in DSF/Cu-induced apoptosis, we treated LNCaP cells with 400 nM DSF/Cu for 24 hours. We found that the apoptosis rate reached to (57.0 ± 5.03)% which was significantly higher than in untreated cells (Figures 2C-2D). We then incubated the cells with chloride channel inhibitors NPPB and DIDS for 20 minutes, following culturing of cells with 400 nM DSF/Cu for 24 hours. The results showed that the apoptosis rate of LNCaP cells decreased to (30.85 ± 5.23)% (NPPB) and (21.81 ± 4.03)% (DIDS). The apoptosis inhibition rate was (39.15 ± 4.90)% for NPPB and (56.74 ± 5.09)% for DIDS (Figure 2E). These findings suggest that DSF/Cu can inhibit the growth and proliferation of LNCaP cells, and chloride channels are likely to participate in the DSF/Cu-induced apoptosis of LNCaP cells.

3.3 | CLC3 siRNA inhibits DSF/Cu-induced chloride currents

In CNE-2Z esophageal cancer cell lines, DSF/Cu mainly activates the CLC3 chloride currents.[17] To explore the relationship between DSF/Cu and CLC3 chloride currents in LNCaP cells, we used CLC3 siRNA to down-regulate CLC3 in LNCaP cells. We conducted western blots to determine the transfection efficiency, and achieved downregulation of CLC3 by (55.49 ± 4.08) %, indicating that CLC3 siRNA treatment successfully downregulated CLC3 expression in LNCaP cells (Figures 3A
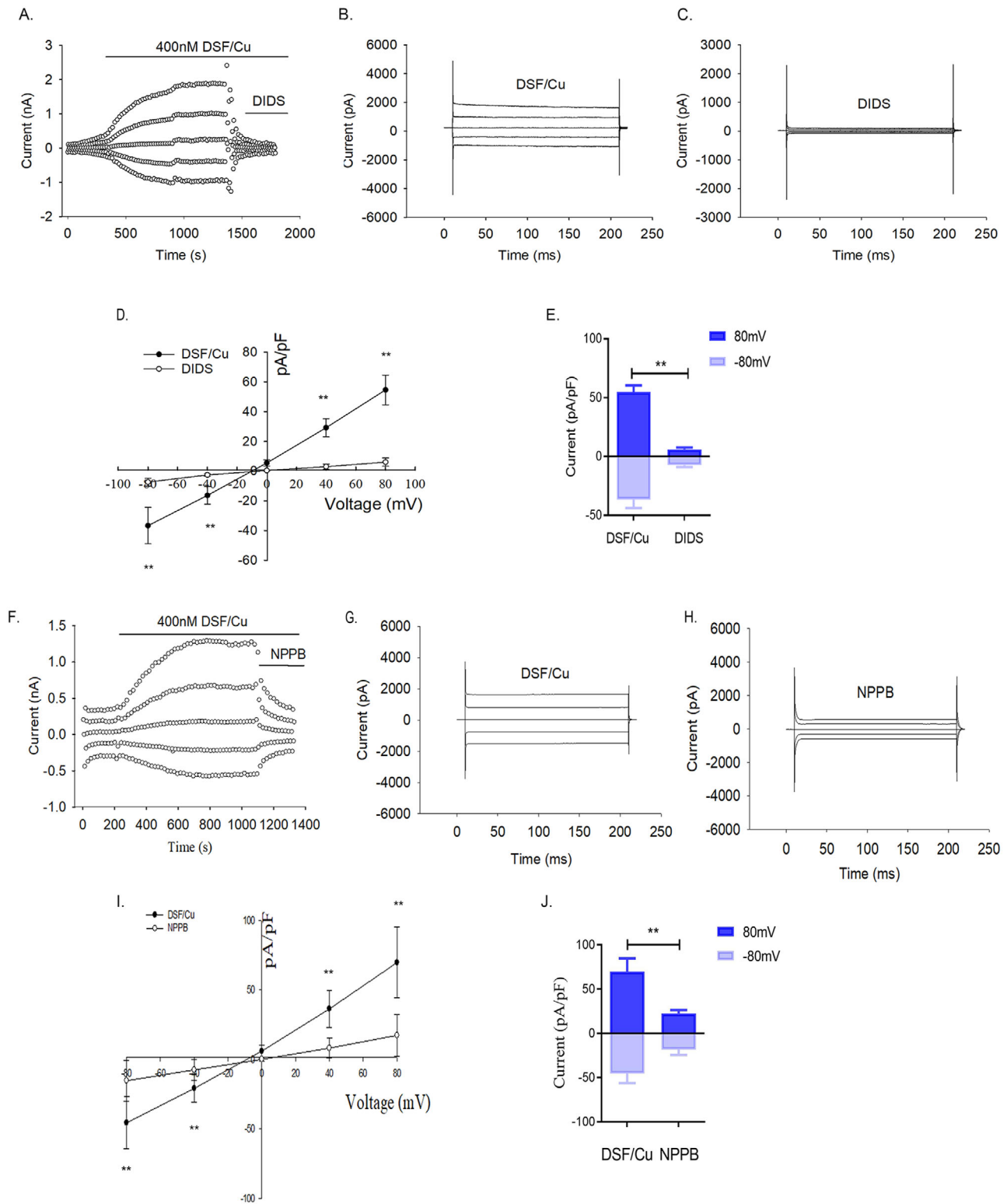
FIGURE 1 DSF/Cu activated chloride currents in LNCaP cells suppressed by NPPB and DIDS. A, Full-process diagram of DSF/Cu-activated LNCaP chloride currents suppressed by DIDS. B, Instantaneous diagram of DSF/Cu-activated LNCaP chloride currents. C, Instantaneous diagram of DSF/Cu-activated LNCaP chloride currents suppressed by DIDS. D, I-V curve of DSF/Cu-activated LNCaP chloride currents suppressed by DIDS. E, Statistics diagram of I-V relationship between DSF/Cu-activated chloride currents and DIDS-suppressed currents (**$P < .01$, n = 3). F, Full-process diagram of DSF/Cu-induced LNCaP chloride currents suppressed by NPPB. G, Instantaneous diagram of DSF/Cu-activated LNCaP chloride currents. H, Instantaneous diagram of DSF/Cu-activated LNCaP chloride currents suppressed by NPPB. I, I-V curve of DSF/Cu-activated LNCaP chloride currents suppressed by NPPB. J, Statistical diagram of I-V relationship between DSF/Cu-activated chloride currents and NPPB-suppressed currents (**$P < .01$, n = 3) [Colour figure can be viewed at wileyonlinelibrary.com]

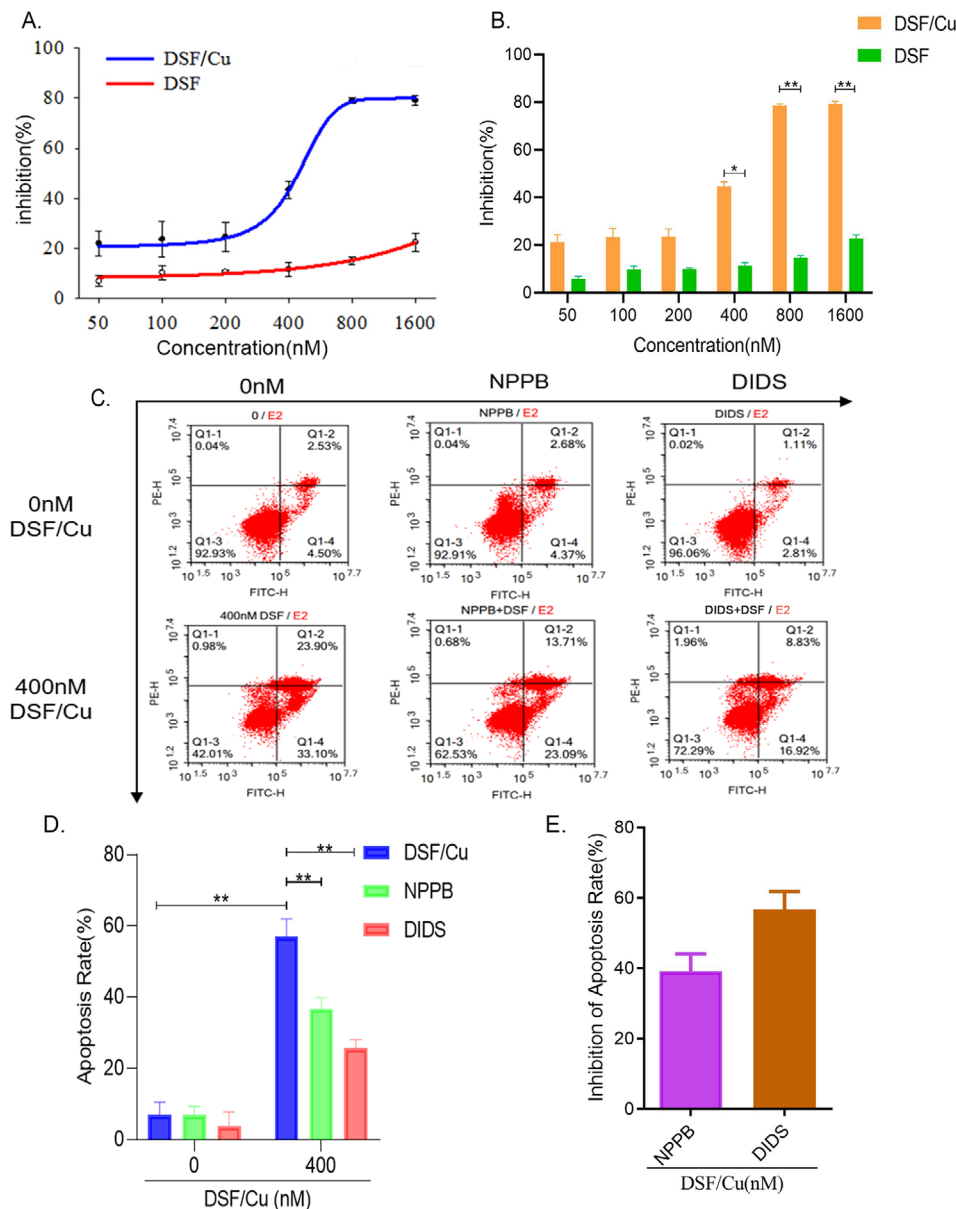**FIGURE 2** DSF/Cu inhibits the growth and proliferation of LNCaP cells and induces apoptosis suppressed by NPPB and DIDS. A, Growth-inhibitory curves of DSF/Cu and DSF at different concentrations. B, Statistical diagram of growth-inhibitory curves of DSF/Cu and DSF at different concentrations (**$P < .01$, *$P < .05$, $n = 3$). C, Scatterplot of flow cytometry detecting the apoptosis rate of LNCaP cells induced by DSF/Cu and NPPB and DIDS (chloride channels inhibitors). D, Statistic graph of apoptosis rate of LNCaP cells induced by DSF/Cu, NPPB, and DIDS (**$P < .01$, $n = 3$). E, Statistic graph of the inhibition rate of NPPB and DIDS inhibiting DSF/Cu-induced apoptosis in LNCaP cells ($P > .05$, $n = 3$) [Colour figure can be viewed at wileyonlinelibrary.com]

and 3B). These CLC3 downregulated cells were detached into a suspension for patch-clamp assays, and their current density was recorded as (19.38 ± 8.91) pA/pF (Figure 3D) while that of the control group was (61.01 ± 7.72) pA/pF (Figure 3C). Moreover, the chloride currents of DSF/Cu-activated LNCaP cells were inhibited by 68% after successful siRNA transfection, indicating that the downregulation of CLC3 suppressed the DSF/Cu-activated chloride currents (Figures 3E-3F). These results verified that the chloride channels in LNCaP cells which were activated by DSF/Cu were indeed CLC3.

3.4 | Tyrosine kinase participates in DSF/Cu activating chloride currents in LNCaP cells

Recent studies have shown that tyrosine kinase may be involved in the DSF/Cu-mediated activation of chloride channels in LNCaP cells,[18] so we focused on tyrosine kinase to elucidate how DSF/Cu activated the chloride currents of LNCaP cells. Treatment with 400 nM DSF/Cu could activate chloride currents of LNCaP cells under a clamping voltage of ± 80 mV, and the current density increased to $(79.72 \pm$
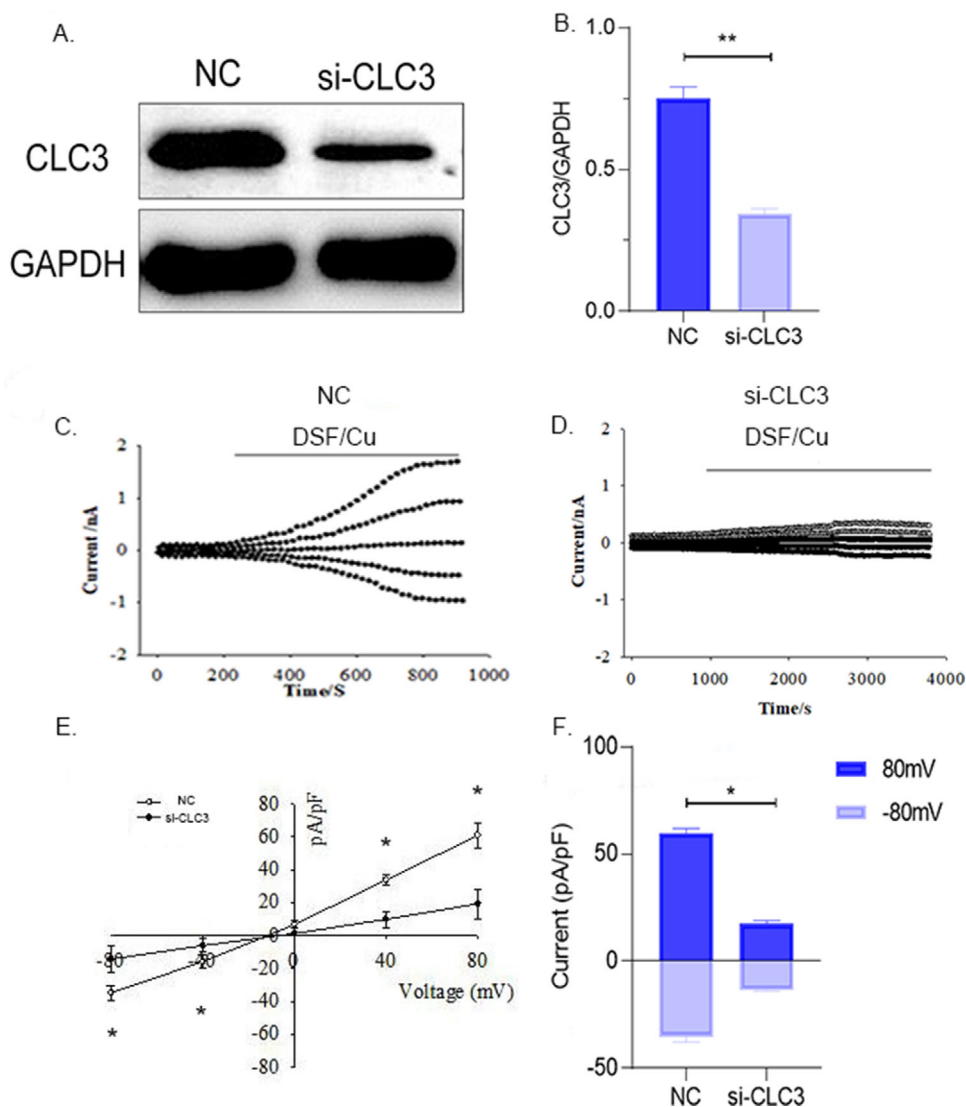
FIGURE 3 Knockdown of the CLC3 chloride channel protein inhibits the activation of currents by DSF/Cu. A, Western blot analysis of protein expression levels. B, Statistical analysis of protein expression (**$P < .01$, n = 3) compared with controls. C, Full process diagram of DSF/Cu-activated NC siRNA-treated LNCaP cells chloride currents. D, Full process diagram of DSF/Cu-activated CLC3 siRNA-treated LNCaP cells' chloride currents. E, I-V curve of DSF/Cu-activated NC siRNA and CLC3 siRNA-treated LNCaP cells' chloride currents. F, Statistic graph of DSF/Cu-activated NC siRNA- and CLC3 siRNA-treated LNCaP cells' chloride current density (*$P < .05$, n = 3) [Colour figure can be viewed at wileyonlinelibrary.com]

17.62) pA/pF (+80 mV), and (−44.72 ± 13.68) pA/pF (−80 mV). We then added a solution containing 30 μM genistein, a highly specific tyrosine kinase inhibitor, to study the role of tyrosine kinase in the activation of chloride channels. Interestingly, the chloride current density activated by DSF/Cu gradually decreased to the background current density level of (14.38 ± 5.65) pA/pF (+ 80 mV) and (−7.84 ± 2.71) pA/pF (- 80 mV). After the currents had stabilized for a period of time and after replacing the extra perfused fluid with DSF/Cu for continued perfusion, a brief increase in cellular currents could be observed before decaying to the level of the background currents, with a second increase in current density of (26.15 ± 3.78) pA/pF (+ 80 mV), which was much smaller than the current density activated by the first perfusion of DSF/Cu (Figures 4A and 4C). This suggested that tyrosine

kinase was likely involved in chloride currents activation of LNCaP in prostate cancer cells.

To further verify the role of tyrosine kinase in DSF/Cu-activated chloride currents, we incubated LNCaP cells with genistein for 30 minutes and then perfused them with 400 nM DSF/Cu solution. The current density of LNCaP cells was (8.31 ± 4.62) pA/pF (+ 80 mV), and there was no difference compared to the background current density of (6.08 ± 3.76) pA/pF. After a period of stability, the cells were perfused with an isotonic solution and then with DSF/Cu solution, after which the current density increased to (23.99 ± 5.77) pA/pF (+ 80 mV) (Figure 4B). This was not significantly different from the current density activated by DSF/Cu after pre-incubation with genistein (Figure 4D).
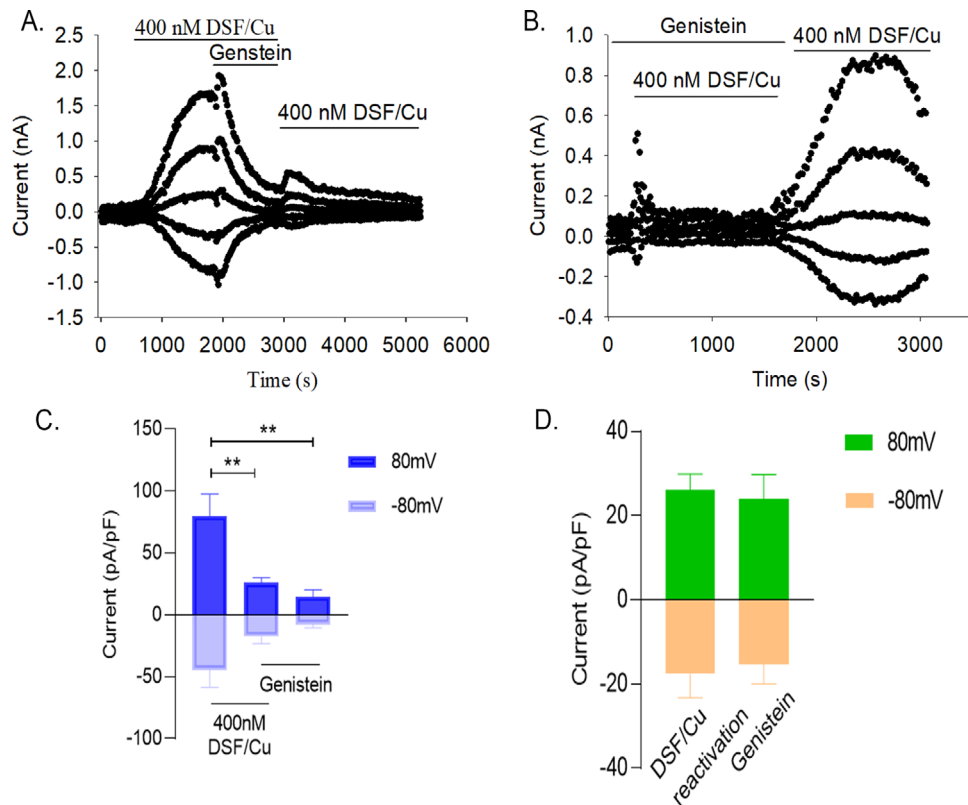
FIGURE 4 DSF/Cu-induced chloride currents suppressed by genistein. A, Full process diagram of DSF/Cu-induced currents and DSF/Cu secondary activated currents suppressed by genistein. B, Full process diagram of DSF/Cu activated currents suppressed by pre-perfusion with genistein. C, Statistic graph of DSF/Cu, genistein and DSF/Cu-reactivated chloride current density (**$P < .01$, n = 3). D, Statistic graph of DSF/Cu perfusion after pre-treatment with genistein and DSF/Cu secondary activated current density ($P > .05$, n = 3) [Colour figure can be viewed at wileyonlinelibrary.com]

3.5 | Co-expression of PTK2B and CLC3 chloride channel

Based on the results, we inferred that tyrosine kinase is closely related to chloride channels in both function and structure in LNCaP cells. Therefore, we performed immunofluorescence assays to study the subcellular localization of CLC3. Blue fluorescence was used to show the nucleus (Figure 5A). CLC3 chloride channel is widely expressed in the cytoplasm, membranes, and nucleoli of LNCaP cells (Figure 5B). We also found that the PTK2B protein and the CLC3 protein were highly co-localized together in the cytoplasm, membranes, and nucleoli of LNCaP cells (Figures 5C and 5D). Further, through protein-protein interaction analysis, we found that the CLC3 protein is closely related to the tyrosine kinase family (Figure 5E). We then simulated a molecular docking model of the CLC3 protein with PTK2B, which suggested that they have potential binding sites (Figure 5F).

4 | DISCUSSION

In recent years, there has been much research on the treatment of prostate cancer, such as endocrine therapy,[19,20] immunotherapy,[21] anti-angiogenic therapy,[22] etc. These emerging therapies have greatly

contributed to the survival of prostate cancer patients. In addition, in recent years, non-coding RNAs have played a key role in a variety of tumors.[23] It has been noted that urine DNA methylation testing helps in the early detection of bladder cancer and monitoring of recurrence.[24] Some lncRNAs and circRNAs are significant in prostate cancer progression as well as prognosis.[25] The mechanisms of tumor regulation are extraordinarily complex, and there are quite a few mechanisms waiting to be discovered.

Our previous results showed that chloride channels are involved in various biological processes in prostate cancer cells. The expression of CLC3 chloride channel in normal controls patients and in prostate cancer patients is significantly different, and the expression of CLC3 is positively correlated with the disease-free survival time of prostate cancer patients. In addition, immunohistochemistry results suggest that the expression of CLC3 in primary tumors is extremely high compared to metastatic tumors, while the histological morphology is similar to neuroendocrine differentiation morphology (data not shown). These results prove that the chloride channels play an important role in the development of prostate cancer. DSF/Cu can also induce the apoptosis of LNCaP cells, and the apoptosis of LNCaP cells induced by DSF/Cu is inhibited after adding chloride channel blockers. DSF/Cu can activate LNCaP cells to produce chloride currents, demonstrating that DSF/Cu induces apoptosis in LNCaP cells through chloride channels.
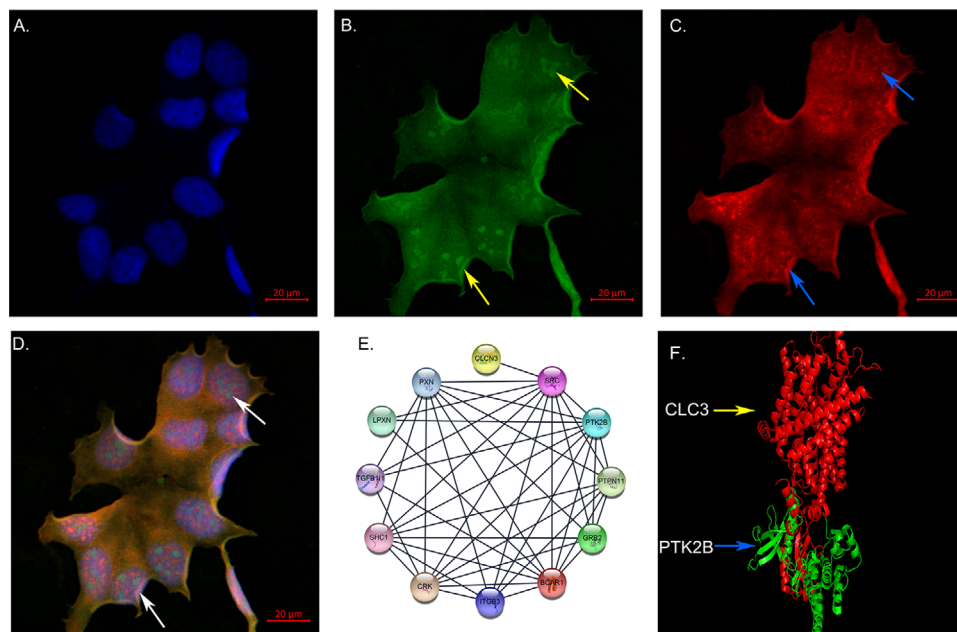
FIGURE 5 Co-expression of tyrosine kinase PTK2B and CLC3. A, Image of Hoechst 33342 staining for nuclei (blue fluorescence) in LNCaP cells. B, Image of CLC3 protein (green fluorescence) in LNCaP cells. C, Image of PTK2B protein (red fluorescence) in LNCaP cells. D, Merged image of three fluorescent images shows that CLC3 protein and PTK2B protein are colocalized. E, Protein-protein interaction network, showing that CLC3 protein and tyrosine kinase family are closely related. F, CLC3 protein and PTK2B protein molecular docking model (red ribbon representing CLC3 protein and green ribbon standing for PTK2B protein) with a match align score 35.000 and RMSD = 13.520 [Colour figure can be viewed at wileyonlinelibrary.com]

In recent years, many existing drugs are being applied in new ways. As a traditional drug for anti-alcoholism treatments, DSF has been constantly exploring as an excellent anti-tumor drug through kinds of new mechanisms.[26–28] ClinicalTrials.gov reports that clinical trials of DSF against non-small cell lung cancer, prostate cancer, and metastatic melanoma have now been completed. Moreover, after chelating divalent metal cations such as zinc ions and copper ions, the therapeutic effect of DSF on tumors is greatly enhanced.[26] DSF can inhibit the proliferation of prostate cancer cells, and copper ions can enhance this effect,[11] which implies that chloride channels may be one of the pathways for DSF/Cu-induced apoptosis of LNCaP cells. However, there is no evidence about how these drugs activate ion channels. It has been suggested that some volume-regulated anion channels are activated through phosphorylation of protein kinases.[29]

Genistein is a highly specific tyrosine kinase inhibitor, and genistein inhibits tyrosine kinase and also closes CLC3 in rat vascular smooth muscle cells.[30] In current experiments, the order of genistein addition had an important effect on whether DSF/Cu could activate the chloride currents of LNCaP cells and on the strength of the currents, indicating that tyrosine kinase is involved in DSF/Cu-mediated activation of the chloride currents in LNCaP cells. Furthermore, DSF/Cu may directly stimulate tyrosine kinase to promote its phosphorylation, and only then activate the chloride currents. The weakened DSF/Cu-activated chloride currents after pre-incubation with genistein also confirmed this hypothesis. However, this mechanism still needs further verification.

Tyrosine kinase is involved in the activation and opening of ion channels. Some studies have found that when the phosphorylation process of tyrosine kinase is blocked, the opening of ion channels is also inhibited, suggesting that tyrosine kinase may activate ion channels by interacting with ion channels after phosphorylation.[31] Another hypothesis is that the activation of tyrosine kinase is related to reactive oxygen species (ROS), and that intracellular redox molecular mechanisms regulate tyrosine kinases and their intracellular signaling at the cell membrane.[32] We found that after treatment with 400 nM DSF/Cu, the expression levels of both PTK2B and CLC3 proteins showed a tendency to increase at first and then decrease over time, but the specific mechanism needs further research. Similar to inhibition of CLC3, treating LNCaP cells with the tyrosine kinase inhibitor genistein could inhibit the apoptosis induced by DSF/Cu. Taking these results together, we conclude that tyrosine kinase has the potential to act as an upstream signal for the chloride channel-induced apoptosis signaling pathway, and the activation of tyrosine kinase leads to downstream opening of the chloride channels, which in turn is involved in biological processes such as cell volume regulation and apoptosis induction.

5 | CONCLUSIONS

The results of this study showed that 400 nM DSF/Cu activates chloride channels in prostate cancer LNCaP cells (mainly CLC3) and plays an active role in inducing apoptosis, and tyrosine kinase has the potential to act as an upstream signal for the chloride channel-induced

apoptosis signaling pathway. The results were promising to provide new perspectives for targeted therapy of prostate cancer.

CONFLICT OF INTEREST

The authors declare that there is no conflict of interest that could be perceived as prejudicing the impartiality of the research reported.

DATA AVAILABILITY STATEMENT

The data that support the findings of this study are available from the corresponding author upon reasonable request.

PERMISSION TO REPRODUCE MATERIAL FROM OTHER SOURCES

Authors are responsible for obtaining permission to reproduce copyrighted material from other sources.

ORCID

Yehui Chen https://orcid.org/0000-0003-0951-2099

REFERENCES

1. Siegel RL, Miller KD, Sauer AG et al. Colorectal cancer statistics, 2020. *CA Cancer J Clin*. 2020;70(3):145-164.
2. Sun G, Chen X, Gong U, et al. Androgen deprivation therapy with chemotherapy or abiraterone for patients with metastatic hormone-naive prostate cancer: a systematic review and meta-analysis. *Future Oncol*. 2019;15(10):1167-1179.
3. Fizazi K, Tran N, Fein L, et al. Abiraterone plus prednisone in metastatic, castration-sensitive prostate cancer. *N Engl J Med*. 2017;377(4):352-360.
4. Daskivich TJ, Howard LE, Amling CL, et al. Competing risks of mortality among men with biochemical recurrence after radical prostatectomy. *J Urol*. 2020;204(3):511-517.
5. Locke J A, Guns E S, Lubik A A, et al. Androgen levels increase by intratumoral de novo steroidogenesis during progression of castration-resistant prostate cancer. *Cancer Res*. 2008;68(15):6407-6415.
6. Gu P, Chen X, Xie R, et al. A novel AR translational regulator lncRNA LBCS inhibits castration resistance of prostate cancer. *Mol Cancer*. 2019;18(1):109.
7. Gu P, Chen X, Xie R, et al. lncRNA HOXD-AS1 regulates proliferation and chemo-resistance of castration-resistant prostate cancer via recruiting WDR5. *Mol Ther*. 2017;25(8):1959-1973.
8. Chen C, Cai Q, He W, et al. AP4 modulated by the PI3K/AKT pathway promotes prostate cancer proliferation and metastasis of prostate cancer via upregulating L-plastin. *Cell Death Dis*. 2017;8(10):e3060.
9. Chen D, Cui QC, Yang H, et al. Disulfiram, a clinically used anti-alcoholism drug and copper-binding agent, induces apoptotic cell death in breast cancer cultures and xenografts via inhibition of the proteasome activity. *Cancer Res*. 2006;66(21):10425-10433.
10. Yang Y, Zhang K, Wang Y, et al. Disulfiram chelated with copper promotes apoptosis in human breast cancer cells by impairing the mitochondria functions. *Scanning*. 2016;38(6):825-836.
11. Iljin K, Ketola K, Vainio P, et al. High-throughput cell-based screening of 4910 known drugs and drug-like small molecules identifies disulfiram as an inhibitor of prostate cancer cell growth. *Clin Cancer Res*. 2009;15(19):6070-6078.
12. Xu X, Xu J, Zhao C, et al. Antitumor effects of disulfiram/copper complex in the poorly-differentiated nasopharyngeal carcinoma cells via activating ClC-3 chloride channel. *Biomed Pharmacother*. 2019;120:109529.
13. Wang W, Mcleod HL, Cassidy J. Disulfiram-mediated inhibition of NF-kappaB activity enhances cytotoxicity of 5-fluorouracil in human colorectal cancer cell lines. *Int J Cancer*. 2003;104(4):504-511.
14. Wang L, Gao H, Yang X, et al. The apoptotic effect of zoledronic acid on the nasopharyngeal carcinoma cells via ROS mediated chloride channel activation. *Clin Exp Pharmacol Physiol*. 2018;45(10):1019-1027.
15. Sawyer JE, Hennebry JE, Revill A, et al. The critical role of logarithmic transformation in Nernstian equilibrium potential calculations. *Adv Physiol Educ*. 2017;41(2):231-238.
16. Elmore S. Apoptosis: a review of programmed cell death. *Toxicol Pathol*. 2007;35(4):495-516.
17. Yang Y, Li M, Sun X, et al. The selective cytotoxicity of DSF-Cu attributes to the biomechanical properties and cytoskeleton rearrangements in the normal and cancerous nasopharyngeal epithelial cells. *Int J Biochem Cell Biol*. 2017;84:96-108.
18. Capurro V, Gianotti A, Caci E, et al. Functional analysis of acid-activated Cl⁻ channels: properties and mechanisms of regulation. *Biochim Biophys Acta*. 2015;1848(1 Pt A):105-114.
19. Hussain M, Fizazi K, Saad F, et al. Enzalutamide in men with nonmetastatic, castration-resistant prostate cancer. *N Engl J Med*. 2018;378(26):2465-2474.
20. Smith MR, Saad F, Chowdhury S, et al. Apalutamide treatment and metastasis-free survival in prostate cancer. *N Engl J Med*. 2018;378(15):1408-1418.
21. Lu X, Horner JW, Paul E, et al. Effective combinatorial immunotherapy for castration-resistant prostate cancer. *Nature*. 2017;543(7647):728-732.
22. Jayson GC, Kerbel R, Ellis LM, et al. Antiangiogenic therapy in oncology: current status and future directions. *Lancet*. 2016;388(10043):518-529.
23. Chen X, Xie R, Gu P, et al. Long noncoding RNA LBCS inhibits self-renewal and chemoresistance of bladder cancer stem cells through epigenetic silencing of SOX2. *Clin Cancer Res*. 2019;25(4):1389-1403.
24. Chen X, Zhang J, Ruan W, et al. Urine DNA methylation assay enables early detection and recurrence monitoring for bladder cancer. *J Clin Invest*. 2020;130(12):6278-6289.
25. Shi J, Liu C, Chen C, et al. Circular RNA circMBOAT2 promotes prostate cancer progression via a miR-1271-5p/mTOR axis. *Aging (Albany NY)*. 2020;12(13):13255-13280.
26. Li Y, Wang LH, Zhang HT, et al. Disulfiram combined with copper inhibits metastasis and epithelial-mesenchymal transition in hepatocellular carcinoma through the NF-κB and TGF-β pathways. *J Cell Mol Med*. 2018;22(1):439-451.

27. Shian SG, Kao YR, Wu FY, et al. Inhibition of invasion and angiogenesis by zinc-chelating agent disulfiram. *Mol Pharmacol*. 2003;64(5):1076-1084.

28. Kim JY, Lee N, Kim YJ, et al. Disulfiram induces anoikis and suppresses lung colonization in triple-negative breast cancer via calpain activation. *Cancer Lett*. 2017;386(1):51-60.

29. Shuba YM, Prevarskaya N, Lemonnier L, et al. Volume-regulated chloride conductance in the LNCaP human prostate cancer cell line. *Am J Physiol Cell Physiol*. 2000;279(4):C1144-C1154.

30. Zhou JG, Ren JL, Qiu QY, et al. Regulation of intracellular Cl-concentration through volume-regulated ClC-3 chloride channels in A10 vascular smooth muscle cells. *J Biol Chem*. 2005;280(8):7301-7308.

31. Huang RQ, Dillon GH. Direct inhibition of glycine receptors by genistein, a tyrosine kinase inhibitor. *Neuropharmacology*. 2000;39(11):2195-2204.

32. Nakashima I, Takeda K, Kawamoto Y, et al. Redox control of catalytic activities of membrane-associated protein tyrosine kinases. *Arch Biochem Biophys*. 2005;434(1):3-10.